Available online at www.sciencedirect.com
SCIENCE DIRECT
Journal of Colloid and Interface Science 299 (2006) 1–13
JOURNAL OF Colloid and Interface Science
www.elsevier.com/locate/jcis

Feature article

The physics of moving wetting lines

Terence D. Blake

8 Hazely, Tring, Herts. HP23 5JH, UK

Received 1 February 2006; accepted 18 March 2006
Available online 27 March 2006

Abstract

Scientists tend to think in terms of their most familiar models. It is not accidental that the earliest descriptions of the moving wetting line and its associated dynamic contact angle were in terms of displaced equilibria (chemists), friction (physicists) and viscous bending of the liquid–vapour interface (engineers and mathematicians). Each of these approaches has progressed since its inception, but, while each reflects a different facet of the underlying physical mechanism, and each offers at least a semi-empirical route to its description, none is complete. There is, as yet, no fully agreed treatment that is consistent with all three viewpoints and provides an effective basis for prediction—though at least one new hydrodynamic approach has emerged that goes some way in this direction. This paper seeks to offer a status report: to briefly review each of the current approaches, to illustrate their successes and limitations as revealed by experiment and simulation, and to suggest ways in which the different aspects of wetting dynamics might be investigated in the future.

Keywords: Dynamic wetting; Contact angle; Hydrodynamics; Molecular dynamics; Coating

1. Introduction

The wetting of a solid by a liquid is a crucial part of many processes, both natural and industrial. For example, in coating a liquid onto a solid it is essential that the liquid dynamically wet the solid surface. However, despite much research over many years, the precise mechanism by which a liquid front advances across a solid remains only partially understood. Thus, our ability to predict wetting behaviour and model processes that are dependent on wetting is significantly restricted [1].

As noted elsewhere [2], this incomplete understanding stems from a number of factors. First, dynamic wetting operates on a scale that extends from the macroscopic to the molecular, while our observations usually involve only macroscopic quantities such as wetting speed, viscosity, surface tension, and the contact angle formed between the liquid and the moving solid, measured at a resolution of no better than several microns. Secondly, the spectrum of natural and industrial processes that involve dynamic wetting is very broad, the materials are diverse and the parameters involved span a very wide range. In industrial coating alone, the solid substrates may range from polymers to metals. The liquids can have viscosities η from less than 1 mPa s (non-aqueous solvents) up to several kPa s (polymers), and surface tensions γ from less than 25 mN m^{-1} (hydrocarbons) to more than 500 mN m^{-1} (liquid metals). The liquid may spread completely on the solid (static contact angle $\theta_S = 0$) or wet it only partially ($\theta_S > 0$). The wetting velocity U can vary from less than 1 μm s^{-1} (droplet spreading) to 10 m s^{-1} or more (curtain coating[1]). Thus, the characteristic capillary number, $\mathrm{Ca} = U\eta/\gamma$, associated with the process can easily span many orders of magnitude.

In contrast with this breadth, systematic experimental investigations of wetting have, with few exceptions, been restricted to relatively narrow velocity ranges, small selections of materials, and capillary numbers that are typically much less than one. Theoretical studies have shown similar limitations, being constrained both by the mathematical methods applied and the difficulty of identifying the physical mechanisms that may operate under the conditions of interest. Indeed most studies have been restricted to the limiting case of small capillary and Reynolds numbers ($\mathrm{Re} = \rho U L/\eta$, where ρ is the density of the

E-mail address: terrydblake@btinternet.com.

[1] Curtain coating is a high-speed coating method in which a freely falling sheet of liquid impinges onto a moving support [2,3].

0021-9797/$ – see front matter
doi:10.1016/j.jcis.2006.03.051

liquid and L the characteristic length of the flow)—which is far from the situation in, for example, a typical coating process. It is, therefore, perhaps hardly surprising that the problem has resisted solution and resulted in a diverse range of viewpoints with, as yet, no true consensus.

In the following sections, the principal theories of dynamic wetting are briefly reviewed and compared with experiment. Strengths and limitations of the theories are considered, as are some of the experimental difficulties. Mention is also made of a relatively new approach in which molecular dynamics (MD) simulations are being applied to dynamic wetting in order to elucidate the underlying physical mechanisms. The paper concludes with some suggestions for future work.

This survey is not intended to be exhaustive; the aim is simply to reflect the author's perspective on current progress. In addition, only those theories and mechanisms that we might expect to be generally applicable are examined. Mechanisms based on special causes, such as evaporation and condensation of the liquid [4], chemical reaction or physical changes in the substrate, are not discussed explicitly. These mechanisms will apply only if special conditions are met; for example, the evaporation/condensation mechanism will be relevant only to sufficiently volatile liquids. As such, it is essentially a "removable" explanation. Furthermore, many of these mechanisms are likely to be relevant only over comparatively long time scales, say in the late stages of the evolution of a liquid drop. They are much less likely to apply at the other end of the scale, e.g. to high-speed liquid coating.

2. The dynamic contact angle and its theoretical interpretation

The main parameters used to quantify the dynamics of wetting are the relative velocity at which the liquid moves across the solid, i.e. the wetting-line velocity U, and the dynamic contact angle θ_D, i.e. the angle formed between the moving liquid interface and the solid surface at the line of three-phase contact (the contact line). The dynamic contact angle is the key boundary condition. Significantly, the experimentally observed dynamic angle generally differs from its static value θ_S and may refer to either an advancing (wetting) or a receding (dewetting) interface. Since solid surfaces are often rough or chemically heterogeneous, even equilibrium contact angles may not be single-valued, but will depend on whether the interface has been advanced or recessed, a phenomenon known as contact angle hysteresis. On such surfaces, wetting lines tend to pin, and when they do eventually move they do so in an unsteady way. Such factors complicate both the measurement and the interpretation of the contact angle. This is especially true on surfaces that react, swell or reorganise in some way on contact with the liquid.

In forced wetting, the contact line is made to move by application of an external force. In such cases, a relationship is expected between θ_D and U for a given system under a given set of conditions. On changing the system or the conditions (e.g. the flow rate in a coating experiment) the precise form of this relationship may change [5,6]. Nevertheless, it is generally observed that advancing angles increase while receding angles decrease with increasing rates of steady contact-line displacement [7,8]. In other words, the contact angle depends on both speed and direction of displacement, i.e. it is velocity-dependent. This is shown schematically in Fig. 1 for a system that also exhibits contact angle hysteresis. While anomalies have been found [8], the relationship between θ_D and U is essentially monotonic. If hysteresis is present, very low, steady wetting-line velocities may not be experimentally accessible due to wetting-line pinning.

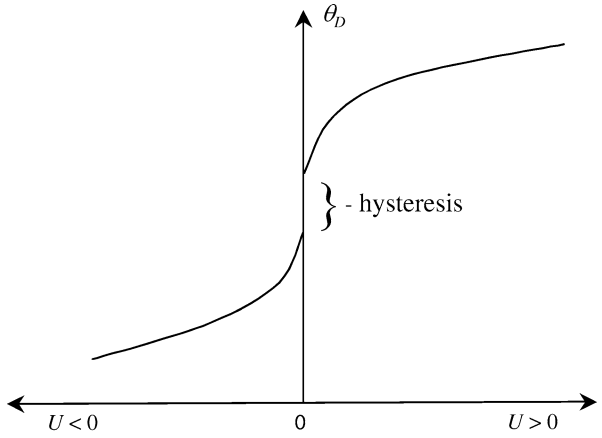

Fig. 1. Velocity-dependence of the contact angle for a partially wetting liquid (after Dussan V [7]).

On the other hand, if a drop of liquid is simply deposited onto a solid it will tend to spread spontaneously under capillary forces alone. Under these transient conditions, the instantaneous dynamic contact angle will relax, decreasing from 180°, at the moment of contact, towards its static value at equilibrium. At the same time, the wetting-line velocity will decrease from its initial value at contact to zero at equilibrium [9].

Whereas forced wetting is about the dynamic balance between the tendency to relax towards equilibrium and some external force driving the system away from it, spontaneous spreading is about the evolution towards equilibrium. Since both forced wetting and spontaneous spreading are examples of moving contact lines, and must therefore involve the same underlying mechanisms, it should be possible to describe them in an equivalent way [10]. Because, by definition, dynamic wetting occurs at a finite rate, possibly with associated changes in the shape of the liquid, but certainly with changes in the wetted area, the processes involved must be thermodynamically irreversible and therefore dissipative. Indeed, the fact that the observed dynamic contact angle is velocity-dependent, and therefore differs from its equilibrium value, is clear evidence of this. Several attempts have been made in the literature to explain the observed behaviour. However, with one important exception [11], to which we will return, these boil down to essentially two approaches, which differ from each other both in terms of their conceptual framework and in their identification of the effective channel of energy dissipation.

One of these two approaches, usually known as the *hydrodynamic theory*, emphasises dissipation due to viscous flow within the wedge of liquid near the moving contact line [7,

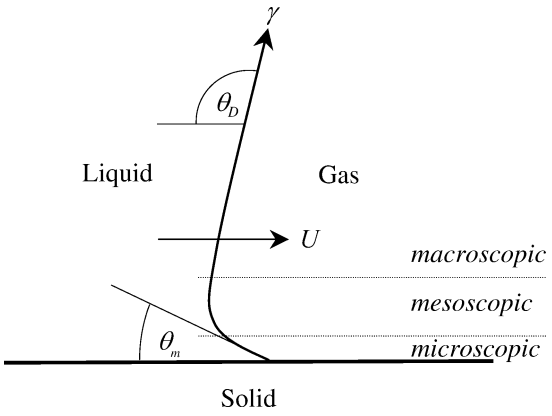

Fig. 2. Viscous bending on the mesoscale for an advancing meniscus.

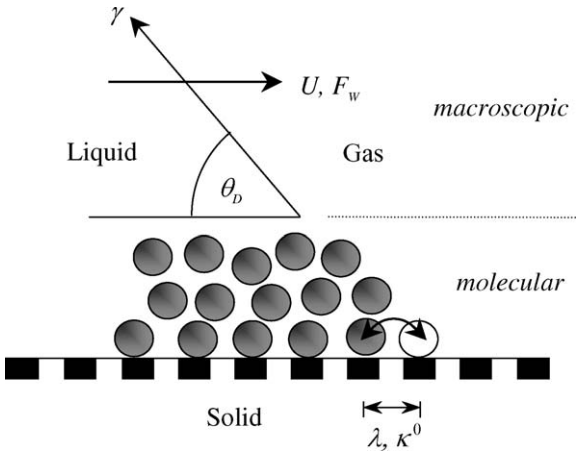

Fig. 3. Dynamic wetting according to the molecular-kinetic theory.

12–22]. Although the various treatments differ in their details, the basic tenet remains the same: changes in the experimentally observed (and therefore macroscopic) dynamic contact angle are attributed to viscous bending of the liquid–gas interface within a mesoscopic region below the scale of observation. The microscopic angle θ_{m} is usually assumed to be governed by short-range intermolecular forces and to retain its static value θ_{S}, though empirical relationships between θ_{m} and U have also been proposed as a way of specifying θ_{m}. Within this hydrodynamic model there are therefore three relevant length scales, as illustrated in Fig. 2.

The other approach originates from the Frenkel/Eyring view of liquid transport as a stress-modified molecular rate process [23,24]. This approach discards dissipation due to viscous flow and focuses instead on that occurring in the immediate vicinity of the moving contact line due to the process of attachment or detachment of fluid particles (molecules) to or from the solid surface, as shown schematically in Fig. 3 [8,25–27]. According to this second model, the channel of dissipation is effectively the dynamic friction associated with the moving contact line [28]. Moreover, it is now the microscopic contact angle that is velocity-dependent and identical with the experimentally observed angle, i.e. $\theta_{\mathrm{D}} = \theta_{\mathrm{m}}$. Thus, there are just two length scales: the molecular scale, where the dissipation occurs, and the macroscopic scale where its effects are seen. This approach is usually termed the *molecular-kinetic theory* (MKT).

Strictly, neither the hydrodynamic nor the molecular-kinetic theory is a *theory*; they are particular *models*, based on broader theoretical systems: on one hand fluid-mechanics, on the other the kinetic theory of liquids. A full discussion of these models is beyond the scope of this review, but it is helpful to outline the basic equations and give some examples of the magnitude of the relevant parameters. More complete overviews and critiques can be found in cited references [1,7,8,11,20,29,30].

2.1. Hydrodynamic theory

As is now well known, the classical hydrodynamic approach to describing flow near a moving wetting line does not result in a physically acceptable solution. Because of the conflict between a contact line that moves and the conventional no-slip boundary condition between a liquid and a solid, stresses are unbounded at the wetting line, and the force exerted by the liquid on the solid becomes infinite [13]. One approach to dealing with this singularity has been to truncate the solution artificially at the molecular scale where the continuum description breaks down [14]. Alternatively, the flow equations and boundary conditions have been modified by relaxing the no-slip condition in the vicinity of the contact line [7,13,16,17]. In this case, the force exerted on the solid is then finite, though the stresses in the liquid remain unbounded. In both cases, the capillary number is presumed small, so that far from the wetting line the liquid–gas interface takes its static shape. It is only on the mesoscale that viscous bending becomes important. The macroscopic dynamic contact angle is then determined by extrapolating the static interface to the solid surface. The flow equations are solved using the method of matched asymptotic expansions.

In its simplest form, the resulting formula describing the change in the dynamic contact angle due to viscous bending of the liquid–gas interface (Fig. 2) may be written in terms of the capillary number as

$$\chi(\theta_{\mathrm{D}}) - \chi(\theta_{\mathrm{m}}) = \mathrm{Ca}\ln\left(\frac{L}{L_{\mathrm{m}}}\right), \quad \theta_{\mathrm{m}} = \theta_{\mathrm{S}}, \tag{1}$$

where the function $\chi(\theta) = \frac{1}{2}\int_0^{\theta}[\hat{\theta}/\sin\hat{\theta} - \cos\hat{\theta}]\,\mathrm{d}\hat{\theta}$. For $\theta_{\mathrm{D}} < 3\pi/4$, the integrand may be approximated by $2\hat{\theta}^2/3$; hence (1) becomes

$$\theta_{\mathrm{D}}^3 - \theta_{\mathrm{m}}^3 = 9\mathrm{Ca}\ln\left(\frac{L}{L_{\mathrm{m}}}\right), \quad \theta_{\mathrm{m}} = \theta_{\mathrm{S}}, \quad \theta_{\mathrm{D}} < 3\pi/4, \tag{2}$$

where L and L_{m} are appropriately chosen macroscopic and microscopic length scales, respectively. The assumption that the local microscopic angle θ_{m} has its equilibrium value is usually taken, on the principle of Occam's razor, as the simplest initial hypothesis to be validated by the success of the model. However, several authors, including Voinov [14], acknowledge that θ_{m} may itself be velocity-dependent. Voinov's paper provides the first analysis leading to Eq. (1). Later treatments differ in their details, but still recover an equation of essentially the same form. Those of Dussan V and co-workers are perhaps the most

illuminating, and Cox's the most complete, giving the solution for the situation in which the receding fluid is a second viscous liquid rather than an inviscid gas [21]. The viscosity ratio of the two fluids is then a key parameter, appearing in the function $\chi(\theta)$. Cox also considers higher order solutions in Ca and the possibility of other sources of dissipation resulting from flow in the inner and outer regions.

In Voinov's treatment, L_m is the distance from the solid at which the solution is truncated. In Cox's analysis, it defines the scale of the inner region where slip is important. Setting $L = 10$ μm, which is the approximate distance from the wetting line at which the contact angle can be measured, and $L_m = 1$ nm, which is of the order of molecular size, then $\ln(L/L_m)$ is estimated to be of the order of 10. Experimental values vary widely, though values of about 10 have often been found, especially for liquids that completely wet the solid. Much larger values have sometimes been reported for non-wetting liquids [30,31], especially at low Ca where one might have anticipated the model would be most effective. These large values are usually thought to be physically unrealistic, since they would appear to require sub-molecular microscopic length scales. The term $\ln(L/L_m)$ also implies that the dynamic contact angle depends to some extent upon the outer (macroscopic) geometry, but in practice the term is usually treated as an adjustable parameter.

While there is no proven slip model, it turns out that the solution is insensitive to the details of the physics within the inner region; so that the only information communicated outward to the intermediate region, where the viscous bending occurs, is the value of θ_m [15]. However, these conclusions arise partly as a consequence of the physical assumptions inherent to the model. A related question is the way in which the intrinsic wettability of the solid influences the dynamic contact angle. Formally, this enters only through the value of θ_S, but, logically, one would also expect it to influence L_m through the strength of the solid–liquid interactions and their impact on slip.

For completely wetting liquids, a precursor film may spread ahead of the meniscus and the hydrodynamic problem is then greatly simplified, since the contact line is no longer directly involved. This has tempted some to invoke hypothetical precursor films as a way of avoiding the contact line problem in computational modelling of coating flows—a procedure that has little to recommend it other than expediency. Precursor films have been observed experimentally, e.g. for spreading drops; however, in reality, they are unlikely to have much relevance at the wetting speeds encountered in industrial processes such as liquid coating. It is also worth pointing out that, except in the case of wetting with a precursor film, there is no direct experimental evidence of viscous bending to the extent required to explain the wide velocity dependence of the dynamic contact angle seen in experiments. Indeed, a comparatively recent and very accurate study of the profile of a liquid meniscus rising between two parallel plates has found significant discrepancies with the predictions of the standard hydrodynamic model at distances $r < 10$ μm from the wetting line, leading to the conclusion that the microscopic contact angle also depends on contact-line speed [32].

If the hydrodynamic model is applied to the spreading of small drops and small contact angles, Eq. (1) leads to simple scaling laws for the base radius R and the dynamic contact angle as a function of time t:

$$R(t) \sim t^{1/10}, \tag{3}$$

$$\theta_D(t) \sim t^{3/10}. \tag{4}$$

These relationships have been widely confirmed for small drops of completely wetting liquids [18,33]. This result is sometimes advanced as a more general demonstration of the validity of Eq. (1) and its underlying assumptions.

2.2. Molecular-kinetic theory

According to the contrasting viewpoint provided by the molecular-kinetic theory [8,25–27], the motion of the contact line is determined by the statistical dynamics of the molecules within a three-phase zone where the solid, liquid and gas phases meet (Fig. 3). On the molecular scale, this zone has a finite size comparable with the thickness of its component interfaces, but is otherwise unspecified within the model. The key parameters are κ^0, the equilibrium frequency of the random molecular displacements occurring within the three-phase zone, and λ, the average distance of each displacement. In its simplest form [26], the model is based on the idea [34] that the velocity-dependence of the dynamic contact angle is due to the disturbance of adsorption equilibria and, hence, to changes in the local surface tensions as the wetting line moves across the solid surface. Thus, the driving force for the contact line to move in a given direction is equal to the out-of-balance surface tension force that arises when equilibrium is disturbed: $F_W = \gamma(\cos\theta_S - \cos\theta_D)$. In this case, λ is supposed to be the distance between adsorption sites on the solid surface. The resulting equation for the wetting-line velocity is then

$$U = 2\kappa^0\lambda \sinh\bigl[\gamma(\cos\theta_S - \cos\theta_D)\lambda^2/2k_BT\bigr], \tag{5}$$

where k_B is the Boltzmann constant and T the absolute temperature. The characteristic frequency κ^0 may be written in terms of the activation free energy of wetting ΔG_w^*:

$$\kappa^0 = \left(\frac{k_B}{h}\right)\exp\left(\frac{-\Delta G_w^*}{Nk_BT}\right), \tag{6}$$

where h and N are the Planck constant and Avogadro number, respectively. While the experimentally determined values of λ are usually of molecular dimensions, those for κ^0 can vary widely, and generally decrease with increasing viscosity. Examples are listed in Table 1.

In a later development of the model [8], a simple relationship between κ^0 and viscosity was proposed:

$$\kappa^0 = \kappa_s^0 h/\eta v_m, \tag{7}$$

where κ_s^0 is the frequency of molecular displacements when retarded only by solid–liquid interactions and v_m is the molecular flow volume. Hence, κ^0 is inversely proportional to viscosity, as found experimentally. More recently, it has been suggested that there is an approximate link between κ_s^0 and the work of

Table 1
Values of parameters obtained by applying the molecular-kinetic theory to experimental data for various systems [8,9]

Liquid–solid system	η (Pa s)	γ (mN m^{-1})	θ_S (°)	λ (nm)	κ^0 (s^{-1})	ζ (Pa s)
Water on PET[a]	0.001	72.4	82	0.36	8.6×10^9	0.01
16% glycerol/water on PET	0.0015	69.7	72.5	0.46	3.6×10^9	0.012
86% glycerol/water on PET	0.104	65.8	65	0.46	3.5×10^7	1.2
Di-*n*-butyl phthalate on PET	0.196	34.3	<5	1.8	1.1×10^5	6.4
Silicone oil on glass [35]	0.958	21.3	0	0.80	2.3×10^5	35.9
Silicone oil on glass [35]	98.8	21.7	0	0.80	2.3×10^3	3580

[a] Polyethelene terephthalate tape.

adhesion between the liquid and the solid, Wa [36]. This leads to

$$\kappa^0 \sim \frac{k_B T}{\eta v_m} \exp(-\mathrm{Wa}). \tag{8}$$

Since both the work of adhesion and the driving force for wetting increase with wettability, Eq. (8) implies that there may be an optimum wettability to maximise the rate of wetting. Evidence for this, and the inverse relationship between κ_s^0 and Wa, can be found in the literature [36].

If the argument of the sinh function is small, Eq. (5) reduces to its linear form

$$U = \kappa^0 \lambda^3 \gamma(\cos\theta_S - \cos\theta_D)/k_B T = \gamma(\cos\theta_S - \cos\theta_D)/\zeta, \tag{9}$$

where $\zeta = k_B T/\kappa^0 \lambda^3$ is the coefficient of wetting-line friction. The idea of a frictional force $G(U)$ at the wetting line was introduced by Voinov [14] to explain local energy dissipation and account for any velocity-dependence of θ_m. However, as he pointed out "The determination of G falls outside the scope of hydrodynamics." The friction coefficient in (9) has the same units as dynamic viscosity. Indeed, the form of the expression for ζ is the same as that given by Eyring for dynamic viscosity, with λ^3 replacing the molecular flow volume v_m—a key parameter in Eyring's analysis [23]. From (8),

$$\zeta \sim \eta\left(\frac{v_m}{\lambda^3}\right) \exp(\mathrm{Wa}). \tag{10}$$

Consistent with this relationship, experimental values of ζ are always larger than the viscosity of the liquid, and appear to increase both with viscosity and the strength of solid–liquid interactions (Table 1).

Notwithstanding these findings, there is no definitive way of predicting the values of λ, κ^0 and ζ for a given solid–liquid system, and so predicting dynamic wetting behaviour from independently measured quantities. In consequence, λ and κ^0 (or ζ) must usually be treated as adjustable parameters and obtained from experiment by curve-fitting procedures. In doing this, great care must be taken that the data are sufficiently extensive and noise free and that the fitting procedures are robust. Statistical techniques such as the Bootstrap method [37] are sometimes applied to analyse the reproducibility of the fits and estimate errors [9]. In particular, a reliable value for λ is crucial, since it appears to the third power in Eq. (9). Another problem intrinsic to the molecular-kinetic model is that there is no link to the wider hydrodynamics of the system. This stems from the fact that all the physics is located within the three-phase zone, which, in the limit of continuum mechanics is simply the contact line. An ad hoc way of making such a link has been proposed [8] in order to partially explain a phenomenon that has become known as *hydrodynamic assist* (see below). Energy supplied by the flow is supposed to augment the surface-tension driving force F_W through a shear stress acting across the three-phase zone. However, this simplistic approach is flawed since it mixes concepts from two very different theoretical frameworks.

Although the molecular-kinetic theory was first developed around a simple adsorption–desorption model of energy dissipation within the three-phase zone, a wide range of alternative activated-rate processes were envisaged from the outset [8,26]. Such mechanistic details can usually only be inferred. But, in a recent intriguing paper on the dynamic contact angle of superfluid liquid helium-4 on caesium, Prevost et al. [38] have reported data consistent with the molecular-kinetic theory, both in terms of the velocity-dependence of the contact angle and the effect of temperature, which offer greater insight. For this system, viscous and frictional forces can largely be discounted, and the observed behaviour would appear to arise as a result of pinning–depinning events as the wetting line moves across a surface containing nanoscale defects. Innovative studies like this point the way to future experiments aimed at elucidating the mechanisms involved when wetting lines move.

2.3. Combined models

Despite their fundamentally different physics and somewhat different predictions, both the hydrodynamic and molecular-kinetic models have been shown to be reasonably effective in describing the experimentally observed behaviour of the dynamic contact angle in a range of systems. But, while Eq. (1) predicts that for small angles $U \propto \theta^3$, Eq. (9) predicts $U \propto \theta^2$. This leads to scaling laws for spreading drops that differ from Eqs. (3) and (4):

$$R(t) \sim t^{1/7}, \tag{11}$$

$$\theta_D(t) \sim t^{3/7}. \tag{12}$$

Careful comparison with experiment therefore appears to offer at least the potential of assessing which model is the more appropriate based on the measured exponent. Nevertheless, with a free choice of the relevant adjustable parameters, good agreement is often obtained with either model. As we will see below, this can make it difficult to arbitrate between them.

In the past, opinion regarding the two models has appeared somewhat polarised. However, a point of view that is gaining increasing ground is the possibility that *both* wetting-line friction and viscous dissipation play a part in determining the dynamic contact angle [14,39–41]. Leaving aside the specific details of the two models, it seems self-evident, on simple thermodynamic grounds, that the microscopic contact angle will be disturbed by movement of the contact line, and equally self-evident that viscous flow in the small wedge of liquid near the contact line is likely to modify the meniscus profile in this region. The real question concerns the relative importance of the two effects and how they can best be described.

Petrov and Petrov [39] have formulated an integrated theory by the simple expedient of combining Eqs. (2) and (5), using (5) to provide the value of θ_m in (2), yielding an equation with three adjustable parameters, λ, κ^0 and $\ln(L/L_m)$. Perhaps not surprisingly, curve-fitting with this equation proved very successful, usually giving better agreement with experimental data than either (2) or (5) alone, especially for receding wetting lines and small contact angles. In addition, the values of the parameters obtained from the analyses appeared reasonable. Similar results have been obtained by others [1,30].

Brochard-Wyart and de Gennes [40] took a different, but more-or-less equivalent approach. Considering dynamic wetting as an irreversible process, the rate of energy dissipation per unit length of the wetting line is the product of the flux U and the out-of-balance surface tension force $\gamma(\cos\theta_S - \cos\theta_D)$. If one then supposes that the total energy dissipation comprises the viscous losses in the (thin) wedge of liquid adjacent to the moving wetting line plus the losses due to wetting-line friction, then, using simplified arguments, one obtains

$$\gamma(\cos\theta_S - \cos\theta_D)U = \frac{6\eta U}{\theta_D}\ln\left(\frac{L}{L_m}\right)U + \zeta U^2, \tag{13}$$

i.e.

$$U = \frac{\gamma(\cos\theta_S - \cos\theta_D)}{\zeta + \frac{6\eta}{\theta_D}\ln\left(\frac{L}{L_m}\right)}. \tag{14}$$

Here, the lengths L and L_m together with the angle θ_D define the wedge of liquid in which viscous dissipation occurs (estimated using the lubrication approximation). The length L characterises the size of the wedge, and L_m the molecular limit where continuum mechanics breaks down. Because the angle of the wedge θ_D occurs in the denominator of the viscous term, viscous dissipation dominates at small angles. Brochard-Wyart and de Gennes interpreted the friction coefficient ζ in terms of the molecular-kinetic theory, Eq. (9).

Using a slightly different method, de Ruijter et al. have derived an equation analogous to Eq. (14) for a spreading drop [41]. Their analysis suggests that a wetting-line friction regime precedes the viscous regime, which becomes dominant only as the contact angle becomes small. A later experimental study appeared to confirm this finding, showing the expected switch in the power law time-dependence, from Eqs. (11) and (12) to Eqs. (3) and (4), as spreading progressed [42].

By combining the molecular-kinetic and conventional hydrodynamic models in this way, these authors have helped us to appreciate that the real physics of the moving wetting line is probably more complex than the individual models would suggest. Nevertheless, the combination is essentially phenomenological, and there is a risk of overparameterisation with consequent lack of robustness in the fitted values. Furthermore, the combined equations remain restricted to flow at very small capillary numbers, say, <0.1. While they may be helpful in quantifying comparatively slow wetting events such as droplet spreading and capillary flow, the equations can be of only marginal value in predicting the outcome of high-speed wetting processes, such as continuous web or fibre coating, where Ca routinely exceeds unity and is frequently much higher [2].

2.4. The Shikhmurzaev model

A more radical and potentially far-reaching approach to modelling the moving wetting line and the dynamic contact angle has been proposed by Shikhmurzaev [11,43]. His continuum treatment accommodates dissipation through standard hydrodynamic channels, but also exploits non-equilibrium thermodynamics to describe dissipation due to the interfacial creation and destruction processes occurring as the contact line moves across the solid surface. One consequence of this is that the microscopic dynamic contact angle is coupled directly to the flow and is not an independent quantity. Analytical expressions can be obtained for certain simplifying conditions, including low capillary and Reynolds numbers, which successfully describe the experimental results found in the literature. Moreover, computational modelling based on this treatment offers the possibility of describing high-speed coating flows in an entirely self-consistent way. Despite this potential, Shikhmurzaev's approach has attracted dogged opposition from some [44], who appear reluctant to admit that there might be anything lacking in the conventional hydrodynamic model.

Full descriptions of Shikhmurzaev's mathematical model, the associated analysis and comparisons with experiment can be found in his publications [11,43]. A more recent paper provides an accessible summary of the analytical solution for the asymptotic case of steady motion at low Ca and low Re, and applies the results to dynamic contact angle measurements with a plunging tape over a wide range of viscosities [45]. Another experimental paper provides a clear outline of the model in relation to curtain coating [6]. Here, we simply summarise the essential features in a qualitative way.

A key element of the model is the fact that as a liquid advances across a solid surface, liquid at the liquid–gas interface becomes transferred to the solid–liquid interface, i.e. there is a material flux from one interface to the other through the contact line. This flux, which has been experimentally confirmed [46], is missing from the conventional model, which has, instead, a stagnation point.[2] Since the properties of the liquid–gas interface (surface tension, material density, structure, etc.) will not in general be the same as those of the solid–liquid interface, some reorganisation of the molecules comprising the interfacial

[2] It is the presence of this stagnation point in the conventional model that leads to the viscous bending of the liquid interface.

regions will be required as the material is transferred. For example liquid–gas interfaces are usually thought to have a sigmoidal density distribution on the scale of the liquid molecules, while the density of liquid adjacent to a solid surface is usually higher and often has a layered profile. Reorganisation from one structure to the other will be diffusive in nature and require some small time to complete, as the liquid–gas interface disappears and the newly created solid–liquid interface attains equilibrium. As a result, at least the solid–liquid interfacial tension will be disturbed from its equilibrium value.[3] Hence, the balance of interfacial tensions at the contact line will be modified, leading to a non-equilibrium value for the local contact angle θ_m. In addition, there will be an interfacial tension gradient, or "relaxation tail," starting at the contact line and extending a distance of order $U\tau$ along the solid–liquid interface, where τ is the characteristic relaxation time of the interface. Since the relaxation process is diffusive, it will depend on the viscosity of the liquid, becoming slower as the viscosity increases. If, on the microscopic length scale, the interface is a layer of characteristic thickness h_i, then

$$\tau \propto \eta h_i^2. \tag{15}$$

In order to relate the interfacial tensions to the local material densities at the interfaces, Shikhmurzaev introduces a linear equation of state. In his notation,

$$\sigma = \gamma\left(\rho_0^s - \rho^s\right), \tag{16}$$

where σ is the interfacial tension, and ρ_0^s and ρ^s are the equilibrium and instantaneous interfacial densities (mass per unit area). The coefficient γ reflects the tendency of the interfacial layer to be rarefied or compressed due to the asymmetric influence of the intermolecular forces from the bulk phase. Hence, γ is an equilibrium property, independent of viscosity and inversely proportional to the liquid compressibility. By introducing Eq. (16), the local variation in θ_m emerges as part of the solution through the mass and momentum balance conditions. While viscous bending of the interface remains possible, its significance is much reduced, leading to the conclusion that it is the variation in θ_m that is largely responsible for the observed variation in θ_D. More complex equations than (16) are possible, but this is the simplest that provides sufficient physics.

Another consequence of the model is that the stress singularity, which usually arises at the contact line as a result of the no-slip boundary condition, is eliminated, not in some arbitrary way, but by the thermodynamic behaviour of the interfaces. Away from the contact line the no-slip condition remains, while in the neighbourhood of the contact line there is apparent slip.

One difficulty with the model is that it introduces additional phenomenological coefficients α and β, linking the flow to, respectively, the surface tension gradient and the shear stress at the interface. It is not easy to see how these coefficients can be determined a priori. Fortunately, order of magnitude estimates are possible, and in the asymptotic solution for low Ca and Re, most of the coefficients can be lumped together in one scaling factor that is a function only of the material properties of the system.

One potential advantage of the Shikhmurzaev model is that it may be used in combination with computational fluid mechanics to simulate complex coating flows at high capillary and Reynolds numbers, without introducing ad hoc concepts such as slip conditions or specifying, in advance, the behaviour of θ_m. That there has not been a flood of papers taking this approach suggests that the problems involved are not trivial.

A benefit that might accrue, if these problems could be overcome, is to explain and model the effect known as hydrodynamic assist. The high-speed limit to coating is usually the onset of dynamic wetting failure, which leads to air entrainment. The term hydrodynamic assist was first coined to emphasise the fact that coating flows may be manipulated to promote wetting and so beneficially postpone air entrainment to higher coating speeds [5]—a fact well known to coating engineers, but not anticipated by the early theories of dynamic wetting.

Visualisation of curtain-coating flows has shown that hydrodynamic assist causes a reduction in the dynamic contact angle for a given contact-line speed [5,6]. This result means that θ_D is not just speed-dependent, but dependent on the details of the flow. This result also implies that all theories and empirical correlations that lead to a single relationship between θ_D and U for a given system must, at best, be incomplete. Presumably, in high-speed coating, it is the reduction in θ_D through changes in the flow that allows the postponement of air entrainment [2,6]. Scaling arguments strongly suggest that the effect is due to a reduction in the local contact angle θ_m, rather than a reduction in the extent of any hydrodynamic bending on an intermediate scale below the optical resolution of the measurements ($\sim$20 μm) [6]. Because, in Shikhmurzaev's model, the dynamic contact angle is part of the solution, one would expect hydrodynamic assist to arise naturally from a properly formulated computational study based around that model.

Intuitively, one can see that the extension of the surface tension relaxation tail along the solid–liquid interface provides a mechanism by which changes in the flow field on an appropriately similar scale can influence the dynamic contact angle. Hydrodynamic assist appears to occur most strongly in coating flows at high Ca where the wetting line is confined within a small geometry. A feature of curtain coating is that the scale of the flow at the foot of the curtain is very small (typically $<$1 mm) and so may approach the scale of the relaxation tail, thus maximising the potential for hydrodynamic assist [2]. A recent computational study of curtain coating has shown that the standard hydrodynamic approach with various slip models is unable to explain the extent of contact angle variation seen experimentally (some 20°) [47]. It remains to be confirmed that Shikhmurzaev's model can succeed where the other fails. Either way, the existence of hydrodynamic assist clearly demonstrates that equations, such as (1) and (5), that predict a unique value of θ_D for a given value of U or Ca are not sufficient to describe the complex phenomenon that is dynamic wetting [6].

[3] During dewetting the solid–vapour and liquid–vapour interfaces will be disturbed.

3. Comparison with experiment

In this section, we examine the success of the models outlined above in describing the experimentally observed behaviour of the dynamic contact angle in a few cases that are quite typical, but have been selected to illustrate the models' respective strengths and limitations.

Experimental results, unless used in a purely descriptive way, have always to be interpreted in terms of a model of some sort, although, of course, it is important not to prejudge the observations in terms of any given model. In dynamic contact angle experiments, it is clearly important to measure the angle as accurately as possible over the widest possible range of wetting-line speeds and angles. Unless this is done, it is difficult to assess whether or not any given theory is truly effective, or merely appears so when fitted to a data set that is too noisy or too small. One should also ensure that sufficient ancillary measurements are made to enable the results to be interpreted as fully and unambiguously as possible. For example, in specifying the liquid, sufficiently accurate measurements of its viscosity (assuming this to be Newtonian, which is not always the case with industrially interesting liquids), surface tension and density will be necessary. Ideally, there will be a range of measurements in which the material properties of the system are varied in a systematic way, with minimum changes to the chemistry of either the liquid or the solid. Similarly, if comparisons are to be made between different flows, it is important to determine the parameters such as geometry and flow rate that properly characterise them. It may also be desirable to ascertain other factors such as the roughness of the solid surface. Taken together, these requirements are very demanding and difficult to achieve. In consequence, we often have to make do with more limited data sets.

Hoffman's data [35] for silicone oils in a glass capillary are plotted in Fig. 4. Although the speed range of the measurements is moderate (about 1 to 400 μm s^{-1}), the two oils have significantly different viscosities (0.96 and 99 Pa s), but essentially the same chemical composition. Hence, the range and consistency of the data when plotted in terms of the capillary number is good. Silicone oils completely wet clean glass, so a precursor film is probable. The curves shown in the figure were obtained by fitting the data to Eqs. (2) and (5). Both the conventional hydrodynamic theory and the molecular-kinetic theory are able to represent the data reasonably well, with sensible values of the fitting parameters. The fit to (2) is slightly better, with an R^2 of 0.994, compared with 0.982 for Eq. (5). The fit to (2) has been truncated at $\theta_D \sim 3\pi/4$ (135°), the accepted limit for the $\chi(\theta)$ approximation [14]. Cox [21] has shown that Eq. (1) in its full form is able to represent the data quite well at higher angles, at least to Ca ∼ 1. Other researchers have found similar results with very similar liquid–solid systems [48]. The good fit to these data is often advanced as evidence for accepting the hydrodynamic theory with $\theta_m = \theta_S$ [49]. In comparison, Eq. (5) does not fit the data well above 140°, predicting larger angles than found experimentally. A corresponding trend has been seen for other high-viscosity liquids and has been ascribed to a form of hydrodynamic assist [8].

Fig. 5 shows the dynamic contact angle plotted as a function of contact-line speed for a polyethelene terephthalate (PET) tape plunging into a pool of 16% aqueous glycerol solution (viscosity 1.5 mPa s) [45]. Here, the curves were obtained by fitting Eqs. (2) and (5) to the data only for speeds of 7 cm s^{-1} and above, with θ_S treated as an additional unknown. The reason for neglecting the low-speed data is given below. When this is done, both the hydrodynamic and molecular-kinetic theories represent the data quite well, with sensible values for the fitting parameters. However, the fit to Eq. (5) is now better, with an R^2 of 0.987 compared with 0.979 for Eq. (2). Moreover, (5) is effective up to angles approaching 180°. Though not checked, it is likely that the hydrodynamic theory would provide an improved fit at large angles if the effect of the gas-to-liquid viscosity ratio were included using the formula given by Cox [21]. In this case the ratio is small but significant (∼0.01), whereas for the high-viscosity silicone oils of Fig. 4 it is effectively zero.

For the aqueous glycerol solutions Ca < 0.2 over the entire range, but the much lower viscosity compared with Hoffman's

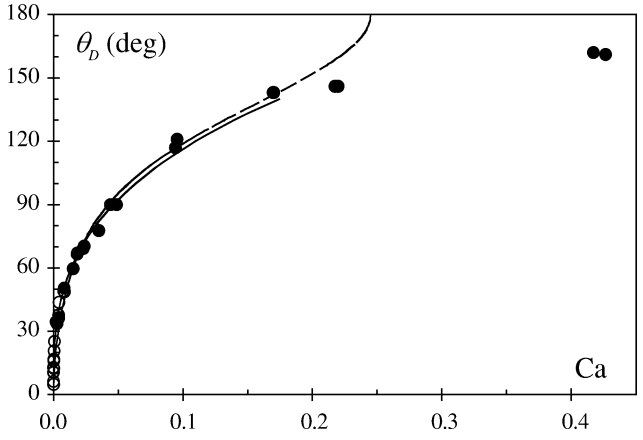

Fig. 4. Dynamic contact angle of silicone oils on glass [35]. Solid curve: hydrodynamic theory, Eq. (2), with $\ln(L/L_m) = 9.3$. Dashed curve: MKT, Eq. (5), with $\lambda = 0.80$ nm, and $\kappa^0 = 2.3 \times 10^5$ and 2.3×10^3 s^{-1} for the 0.96 and 99 Pa s oils, respectively. $\theta_S = 0$ in both cases.

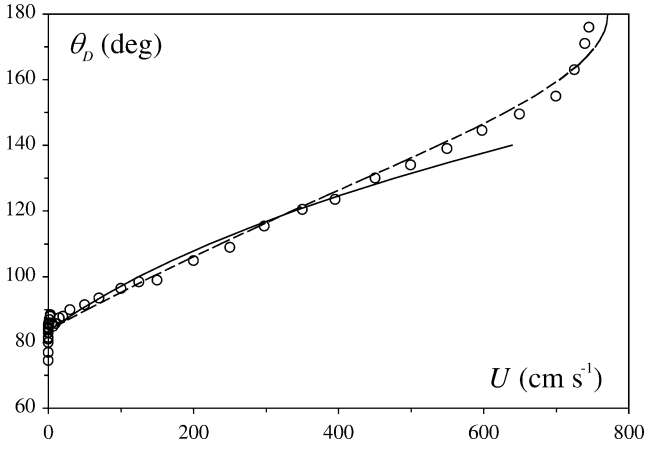

Fig. 5. Dynamic contact angle of 1.5 mPa s aqueous glycerol solution on PET at 22 °C [45]. Solid curve: hydrodynamic theory, Eq. (2), with $\ln(L/L_m) = 9.2$ and $\theta_S = 83°$. Dashed curve: MKT, Eq. (5), with $\lambda = 0.39$ nm, $\kappa^0 = 4.8 \times 10^9$ s^{-1}, and $\theta_S = 84°$.

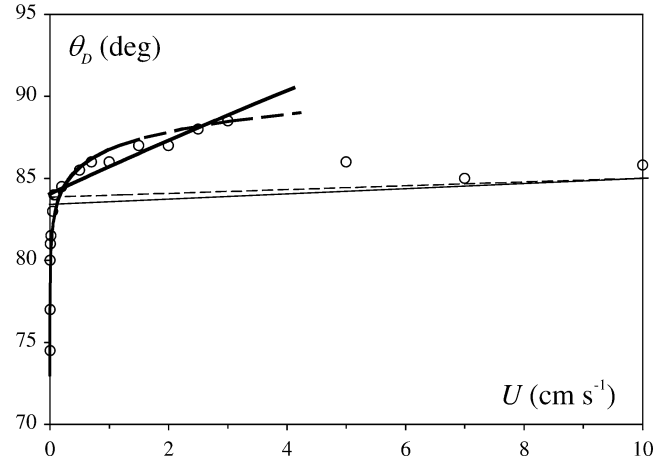

Fig. 6. Low-speed data from Fig. 5 for 1.5 mPa s aqueous glycerol solution on PET. Heavy solid line: hydrodynamic theory, Eq. (2), with $\ln(L/L_m) = 97$ and $\theta_S = 84°$. Heavy dashed curve: MKT, Eq. (5), with $\lambda = 2.1$ nm, $\kappa^0 = 6.2 \times 10^2$ s^{-1}, and $\theta_S = 72.5°$ (measured static advancing angle). The two lighter lines are the fits to the high-speed data shown in Fig. 5.

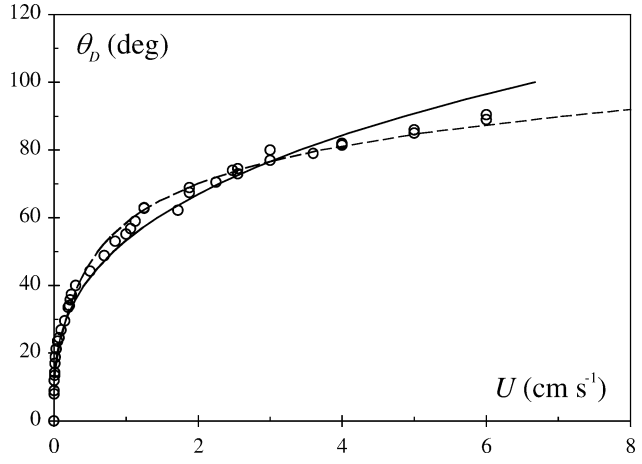

Fig. 7. Dynamic contact angle of di-*n*-butyl phthalate on PET at 55 °C ($\eta = 6.6$ mPa s, $\gamma = 30.9$ mN m^{-1}). Solid curve: hydrodynamic theory, Eq. (2), with $\ln(L/L_m) = 41.5$ and $\theta_S = 10°$. Dashed curve: MKT, Eq. (5), with $\lambda = 1.0$ nm, $\kappa^0 = 1.8 \times 10^5$ s^{-1}, and $\theta_S = 10°$. The measured value of θ_S was small, <5°, but probably not zero. (Data obtained by G.N. Batts and T.D. Blake, Kodak Limited R & D.)

silicone oils results in much higher wetting speeds. However, it is perhaps the data at low speeds (and very low Ca) that are more interesting. The dynamic contact angles in Fig. 5 were obtained over a speed range in excess of 5 orders of magnitude (30 μm s^{-1} to 745 cm s^{-1}), using specially designed apparatus. At speeds up to about 3 cm s^{-1} (Ca $\sim 6 \times 10^{-4}$), the angle follows a very steep curve compared with that found at higher speeds. Immediately above this lower speed range, the angle actually falls by about 5°, and the shallower curve then appears to start at about 7 cm s^{-1} (see Fig. 6). The fall in the contact angle is associated with unsteady motion of the wetting line, which is absent at both higher and lower speeds. A similar effect has been reported for water and, to a lesser extent, for more viscous aqueous glycerol solutions on PET, and has been attributed to a change in the physical mechanism by which the wetting line advances across the solid surface [8]. This discontinuity is the reason why the curves in Fig. 5 were obtained by fitting only the data for speeds of 7 cm s^{-1} and above, and treating θ_S as an additional fitting parameter. Leaving to one side the question of what causes the transition, the low-speed data still cover some 3 orders of magnitude in wetting-line speed and may, therefore, be treated independently.

The result of fitting the low-speed data from Fig. 5 to Eqs. (2) and (5) is shown in Fig. 6. Evidently the fit to (2) is very poor, even if θ_S is adjusted. Moreover, the magnitude of $\ln(L/L_m)$ is physically quite unacceptable. Indeed, with $\theta_S = \theta_m$ and an acceptable value of $\ln(L/L_m)$, Eq. (2) is intrinsically unable to account for such steep changes in θ_D at such low Ca ($<10^{-3}$) unless θ_S is small (which is not the case here) [50]. Another problem is that our understanding of slip suggests that, due to weaker solid–liquid interactions, slip is more likely for partially wetting liquids than for ones that completely wet the solid [51]. This should lead to reduced values of $\ln(L/L_m)$, not substantial increases. In contrast, the molecular-kinetic equation provides a good fit to the data of Fig. 6 based on the measured value of θ_S, and gives acceptable values of κ^0 and λ. These are very different to those obtained with the high-speed data: κ^0 is some 7 orders of magnitude smaller and λ about 5 times larger. However, this simply reflects the very steep dependence of θ_D on U or Ca found experimentally. Within the context of the model, it implies a very strong interaction between the liquid and a relatively low density of adsorption sites on the solid that are resolved only when the wetting line is moving slowly. The literature suggests that small values of κ^0 and comparatively large values of λ are not unusual when the molecular-kinetic theory is applied to dynamic contact angles measured at low speeds [30,31].

Another comparison of the effectiveness of the hydrodynamic and molecular-kinetic equations is shown in Fig. 7. Here, the data are for di-*n*-butyl phthalate on PET at 55 °C. They were obtained by G.N. Batts and the author using the plunging tape method as part of a study to investigate the influence of temperature on the dynamics of wetting. As can be seen, both Eqs. (2) and (5) provide very good fits if some latitude is given to θ_S. That for (5) is marginally better than that for (2), with $R^2 = 0.994$ compared with 0.986. The fits are only slightly worse if θ_S is forced to take a value of zero. The fitting parameters for Eq. (5) also have reasonable values, but the value of $\ln(L/L_m)$ for Eq. (2) is again physically unacceptable. It may be relevant that with this system, there is also a discontinuity in dynamic wetting behaviour, with a small drop in the contact angle within a well-defined transition region. At 55 °C, the low-speed regime extends to $U \sim 6$ cm s^{-1} and $\theta_D = 90°$. The experimental data start at 30 μm s^{-1} and $\theta_D = 8°$, which gives a speed range of at least 3 orders of magnitude. The high-speed regime extends to about 97.6 cm s^{-1}, at which θ_D approaches 180°. Outside the transition region, wetting is steady in both regimes, with the contact angle increasing smoothly with speed.

Fig. 8 shows a further set of measurements made by the author using the plunging tape method; in this case for 86% aqueous glycerol, viscosity 0.104 Pa s, on smooth poly-

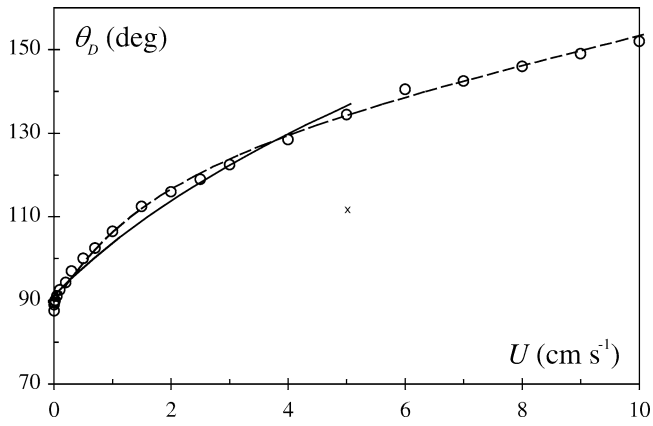

Fig. 8. Dynamic contact angle of 0.104 Pa s aqueous glycerol solution on polyethylene coated paper at 22 °C ($\gamma = 64.1$ mN m^{-1}). Solid curve: hydrodynamic theory, Eq. (2), with $\ln(L/L_m) = 11.3$ and $\theta_S = 91°$. Dashed curve: MKT, Eq. (5), with $\lambda = 0.67$ nm, $\kappa^0 = 6.3 \times 10^6$ s^{-1}, and $\theta_S = 89°$. The measured value of θ_S was 88° (static advancing angle).

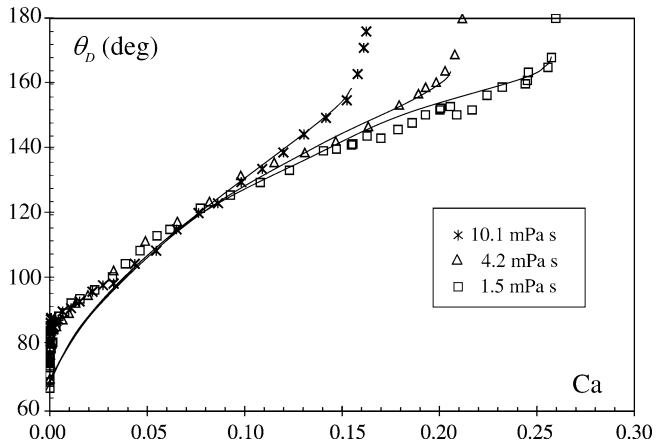

Fig. 9. Dependence of the dynamic contact angle on the capillary number for 1.5, 4.2 and 10.1 mPa s glycerol solutions on PET. Theoretical curves obtained using the Shikhmurzaev model with a constant set of fitting parameters [45].

ethylene coated paper. The data cover speeds from 30 μm s^{-1} to 10 cm s^{-1}. The quality of the fit to Eq. (5) is very good, with $R^2 = 0.996$, and sensible parameters. That to (2) is reasonable, with $R^2 = 0.985$ and a physically acceptable value for $\ln(L/L_m)$. With this system, there was no evidence of any discontinuity over the entire speed range.

The results presented above are fairly representative of other comparisons to be found in the literature where sufficiently extensive data are available. They show the molecular-kinetic approach to be, perhaps, a little more flexible and adaptable compared with the standard hydrodynamic theory. But they also illustrate how unsafe it may be to draw conclusions as to the general validity of either model simply on the basis of the quality of the fits to the equations or the values of the resulting parameters. This is especially true if the data is restricted to a narrow class of liquids. An exception is the case where one viscous liquid displaces another. Here, serious discrepancies have been found if the viscous bending model is used alone [48,50], whereas adequate fits have been obtained with the molecular-kinetic equations [26]. Another exception is in the case of high-viscosity liquids at high contact angles, where the molecular-kinetic model predicts larger angles than found experimentally and a hydrodynamic influence is postulated [8]. A comparable problem exists at small receding angles when viscous dissipation appears to become dominant [39,42]. Furthermore, in those cases where the viscous-bending model predicts submolecular slip length-scales, we must suppose that either the model is invalid or that some additional mechanism is at work that makes θ_m dependent upon wetting-line speed. Overall, it seems that neither model is universally applicable, but that *both* hydrodynamic and molecular mechanisms are at work: that viscous bending may occur, but that θ_m is also speed-dependent.

This brings us directly back to Shikhmurzaev's model. At present, his theoretical approach appears to be uniquely able to describe experimental data in an entirely self-consistent way, without recourse to ad hoc concepts. Shikhmurzaev's publications [10,11,43,45] have shown many examples of how the asymptotic version of his model can account for the dynamic contact angle behaviour found in an exceptionally wide range of systems, from Hoffman's oils on glass [35] and Fermigier and Jenffer's data on two-liquid systems [48], to molten glass on platinum [19].

Here we will look at just one example, based on the dynamic contact angle measurements for three aqueous glycerol solutions on PET reported by Blake and Shikhmurzaev [45]. The data for one of these systems have already been presented in Fig. 5. The combined set, for 1.5, 4.2 and 10 mPa s glycerol solutions, is shown in Fig. 9, together with the fits obtained by applying Shikhmurzaev's equations using a constant set of three, viscosity-independent adjustable parameters (see [45] for details). It is worth stressing that the fitted parameters contain only those material properties that one would expect to remain fixed if the viscosity alone were changed. The differences in the curves enters through the viscosity ratio between the gas and the liquid, which varies from 0.01 to 0.0015 and comes into play as the dynamic contact angle approaches 180°. In fitting the data, no account was taken of the possibility of a change in the mechanism of dynamic wetting at low speeds, so the fit is not good in this region. However, the data could just as well have been fitted selectively, as in Figs. 5 and 6 above; in which case much closer agreement would have been achieved. Moreover, as shown in the original publication, the same set of fitting parameters is able to describe, with good precision, not only these results, but also those obtained with solutions of progressively higher viscosity up to 672 mPa s—a range of nearly three orders of magnitude.

Analysis of the fitted parameters gives values of the interfacial relaxation time τ that range from 5.6×10^{-9}–1.9×10^{-8} s for the 1.5 mPa s solution, to 2.5×10^{-6}–8.3×10^{-6} s for the 672 mPa s solution. These values are not too different to the relaxation times $1/\kappa^0$ obtained by fitting Eq. (5) collectively to the same data with λ held constant: 3×10^{-9}–1.3×10^{-6} ($\lambda \approx 0.6$ nm). As previously noted [45], this agreement suggests a possible correlation between κ^0 and τ that requires further research, possibly using molecular dynamics, to which we now turn.

4. Molecular dynamics

Molecular dynamics (MD) is one of the few tools available to explore the molecular details of wetting. However, it is only within the last 20 years that computer power has grown sufficiently to make it practical to compute the dynamics of quasi-macroscopic systems and so simulate a real experiment. The obvious strength of the technique in the study of dynamic wetting is that it can delve into the process at the molecular level, while at the same time simulating the macroscopic behaviour of the system as a whole. Another advantage is that it can provide a level of control that would be very difficult or even impossible to achieve in physical experiments. For example, the degree of wetting, as reflected by θ_S, can be adjusted selectively simply by changing the solid–liquid coupling—something that could be done in a real experiment only by changing the nature of the solid or the liquid and, thus, many other physicochemical parameters. On the negative side, most practical simulations are still restricted to small systems of the order of a few tens of nanometres and short times of the order of a few nanoseconds. The simulations are therefore subject to significant thermal and statistical fluctuations. Full details of the methods can be found in the cited references, and we will therefore review just the main conclusions that impact our understanding of dynamic wetting.

The first detailed MD study of the static contact angle known to the author is that of Saville [52]. However, it was not until the groundbreaking publications of Koplik et al. [53,54] and Thompson et al. [55,56] that convincing simulations of dynamic contact angles and moving wetting lines became available. These simulations, which involved Lennard–Jones liquids and several thousand "molecules" in Poiseuille and Couette flow, appeared to exhibit continuum behaviour at the system level. The simulations were for liquid–liquid displacement, rather than liquid–vapour.

The Poiseuille studies [53,54] confirmed the no-slip condition at the solid–liquid interface under normal conditions, but suggested that slip might be occurring in the vicinity of the moving wetting line, though the details could not be ascertained. The dynamic contact angle was seen to vary with wetting-line speed, with advancing angles increasing and receding angles decreasing, as observed experimentally. Furthermore, it was the *local* contact angle θ_m, as defined on a molecular scale, which was seen to vary.

The Couette studies [55,56] also confirmed the no-slip condition at the solid–liquid interface and were able to quantify the region of apparent hydrodynamic slip, suggesting that it was restricted to a zone of about 1.8σ around the moving wetting line, where σ is the molecular length scale of the liquid. However, in this case it was concluded that θ_m was constant and equal to θ_S, although this is not obvious from the published images (Figs. 8b and 8c in [56]). Furthermore, the method of assessing θ_D near the centre of the flow at a fixed distance of 6.38σ from the contact line seems arbitrary and unrelated to what one would do in physical experiments. With θ_D measured in this way, Thompson et al. found good agreement between their results and the standard hydrodynamic model, but with physically unrealistic values of $\ln(L/L_m)$ for the stronger of the two solid–liquid interactions modelled. This, it was suggested, was due to what amounts to energy dissipation in the slip region.

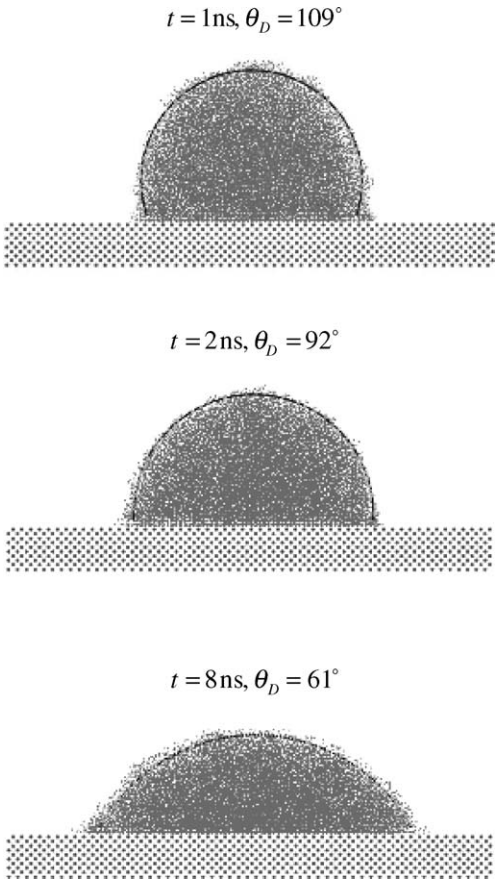

Fig. 10. Sequence of three snapshots, taken from a large-scale MD simulation of a liquid drop spreading on a solid surface. The liquid has an effective viscosity of 0.035 mPa s and surface tension 10.7 mN m^{-1}. The solid lines are circular fits to the liquid interface. Images kindly provided by David Seveno, Centre for Research in Molecular Modelling, University of Mons-Hainaut, Belgium.

More recent, large-scale MD simulations of spreading liquid drops [28,57], spreading cylinders [58], capillary imbibition [59,60] and the dynamic wetting of fibres [61] seem to confirm what the Poiseuille studies initially suggested: that θ_m is not constant and equal to θ_S, but varies with wetting-line speed in a systematic way. Its value very close to the solid appears to be slightly smaller than that θ_D when this is assessed by methods that mimic macroscopic experiments, e.g. by fitting a circular profile to a spreading drop. This is thought to be due to entropic effects [28]. However, for partially wetting liquids, none of the studies reveals any evidence of viscous bending of the liquid–gas interface, despite the fact that there is large variation in θ_D for a variation in Ca that is similar to that found experimentally.

By way of illustration, Fig. 10 shows a sequence of three snapshots taken from a large-scale simulation of a spreading drop. The snapshots are at 1, 2 and 8 ns after initial contact between the pre-equilibrated drop and the solid surface. The simulation involved a liquid droplet comprising 25,600 atoms in 16-atom chains on a realistic solid of 60,500 atoms. The choice of Lennard–Jones coupling constants and other parameters was

such that at long times (>13 ns) the contact angle relaxed to an equilibrium value of 56°, i.e. the liquid was partially wetting. The solid lines are circular fits to the liquid interface from which the contact angles were determined. The progressive reduction in $\theta_D \approx \theta_m$ with time is evident. During this period the capillary number fell from an initial value of about 0.2, which is what one would expect in a real experiment.

As experience and computer power has increased, the simulations have become increasingly realistic. For example they now involve liquid molecules comprising chains up to 40 atoms, which reduces evaporation and also allows the effects of changing viscosity to be studied. In general, the simulations appear to behave globally as macroscopic physical systems. It is therefore all the more intriguing that the dynamic contact angle behaviour has been found to follow that predicted by the molecular-kinetic theory. Moreover, the molecular displacement frequencies at the solid–liquid interface, which can be ascertained directly from the simulations, agree closely with those obtained by fitting Eq. (5) to the dynamic contact angle data [28,61]. This suggests that the molecular-kinetic model has some underlying validity.

What has not yet been demonstrated is a variation in the solid–liquid interfacial tension, γ_{SL}, near the moving contact line. By invoking the dynamic analogue of Young's equation, a local change in γ_{SL} can be inferred from the change in the contact angle from its equilibrium value, but the distance over which the change might propagate along the solid–liquid interface cannot. At equilibrium, the three-phase zone in the simulations appears to be just a few σ in extent, as expected. Confirmation that the interfacial transition region extends further along the solid–liquid interface during flow would provide support for the "relaxation tail" in the Shikhmurzaev model.

5. Conclusions and future directions

As we have seen, it is difficult to draw firm conclusions as to the origins of the dynamic contact angle from the results of simple dynamic contact angle measurements. They provide useful data, but are not definitive. If further studies of this type are to be pursued, then they should be on well-characterised solids that are smooth and homogeneous to avoid the ambiguities of contact angle hysteresis—unless, of course, it is the effect of controlled roughness and heterogeneity that is being explored. In addition, they should be carried out over the widest possible range of conditions, and in varying geometries. More adventurous and discriminating studies such as those reported for superfluid liquid helium-4 on caesium [38] are also desirable, as are any others aimed at illuminating the causes of dynamic contact angle effects in special cases. At high capillary numbers, the origin of hydrodynamic assist needs to be confirmed by visualising more coating flows. The effects of replacing air with a vacuum should be studied in more detail. Already, there is a strong indication that a reduction in air pressure leads to the postponement of air-entrainment [62], but no results have been published on the dynamic contact angle under the same conditions. Such measurements might provide an indication of the mechanisms at work.

Computational fluid dynamics (CFD) applied to coating flows has tended to concentrate on global effects. The contact-line boundary conditions have often been chosen for computational convenience rather than on the basis of a valid physical model. Only part of the reason for this can be that the model is not yet fully established. In particular, it is highly desirable to see Shikhmurzaev's model properly evaluated.

Molecular dynamics simulations have progressed a long way in answering our questions concerning the molecular details of dynamic wetting, at least for simple Lennard–Jones liquids on simple but realistic solids. This work needs to be continued and developed as computational speed and refinements to the code accrue. Possible goals include: a more detailed investigation of the three-phase zone and its comparison with the general solid–liquid and liquid–vapour interfaces, with a view to testing the Shikhmurzaev model; extending simulations to higher Ca in forced wetting and dewetting situations, so that there is an increased probability of detecting effects due to viscous dissipation and hydrodynamic assist; and the introduction of more complex intermolecular forces in order to study structural effects. Two-liquid systems should also be examined in depth to investigate the effects of competitive wetting and viscosity ratio.

Evidently, dynamic wetting remains a fertile area of research, with much still left to investigate and opportunities for progress in both theory and experiment that are likely to have significant practical impact.

Acknowledgments

All the mistakes in this review are my own. Nevertheless, in coming to my conclusions, I have benefited greatly from discussions with many people over many years. I would like to single out the late Mike Haynes, Jordan Petrov, Kenneth Ruschak, Andrew Clarke, Yulii Shikhmurzaev, John Ralston, and Joel De Coninck. The stimulation provided by others with differing viewpoints is also much appreciated.

References

[1] T.D. Blake, K.J. Ruschak, in: P.M. Schweizer, S.F. Kistler (Eds.), Liquid Film Coating, Chapman & Hall, London, 1997, p. 63.
[2] T.D. Blake, R.A. Dobson, K.J. Ruschak, J. Colloid Interface Sci. 279 (2004) 198.
[3] K. Miyamoto, Y. Katagiri, in: P.M. Schweizer, S.F. Kistler (Eds.), Liquid Film Coating, Chapman & Hall, London, 1997, p. 463.
[4] P.C. Wayner Jr., Langmuir 9 (1993) 294.
[5] T.D. Blake, A. Clarke, K.J. Ruschak, AIChE J. 40 (1994) 229.
[6] T.D. Blake, M. Bracke, Y.D. Shikhmurzaev, Phys. Fluids 11 (1999) 1995.
[7] E.B. Dussan V, Ann. Rev. Fluid Mech. 11 (1979) 371.
[8] T.D. Blake, in: J.C. Berg (Ed.), Wettability, Dekker, New York, 1993, p. 251.
[9] M.J. de Ruijter, J. De Coninck, T.D. Blake, A. Clarke, A. Rankin, Langmuir 13 (1997) 7293.
[10] Y.D. Shikhmurzaev, Phys. Fluids 9 (1997) 266.
[11] Y.D. Shikhmurzaev, J. Fluid Mech. 334 (1997) 211.
[12] R.J. Hansen, T.Y. Toong, J. Colloid Interface Sci. 37 (1971) 196.
[13] C. Huh, L.E. Scriven, J. Colloid Interface Sci. 35 (1971) 85.
[14] O.V. Voinov, Fluid Dyn. 11 (1976) 714.
[15] E.B. Dussan V, J. Fluid Mech. 77 (1976) 665.

[16] C. Huh, S.G. Mason, J. Fluid Mech. 81 (1977) 401.
[17] (a) E.B. Dussan V, J. Fluid Mech. 77 (1976) 665;
(b) C.G. Ngan, E.B. Dussan V, J. Fluid Mech. 209 (1989) 191.
[18] L.H. Tanner, J. Phys. D Appl. Phys. 12 (1979) 1473.
[19] L.M. Hocking, A.D. Rivers, J. Fluid Mech. 121 (1982) 445.
[20] P.G. de Gennes, Rev. Mod. Phys. 57 (1985) 827.
[21] R.G. Cox, J. Fluid Mech. 168 (1986) 169.
[22] E.B. Dussan V, E. Rame, S. Garoff, J. Fluid Mech. 230 (1991) 97.
[23] S. Glasstone, K.J. Laidler, H.J. Eyring, The Theory of Rate Processes, McGraw–Hill, New York, 1941.
[24] J.I. Frenkel, Kinetic Theory of Liquids, Oxford Univ. Press, Oxford, 1946.
[25] B.W. Cherry, C.M. Holmes, J. Colloid Interface Sci. 29 (1969) 174.
[26] T.D. Blake, J.M. Haynes, J. Colloid Interface Sci. 30 (1969) 421.
[27] E. Ruckenstein, C.S. Dunn, J. Colloid Interface Sci. 59 (1977) 135.
[28] M.J. de Ruijter, T.D. Blake, J. De Coninck, Langmuir 15 (1999) 7836.
[29] S.F. Kistler, in: J.C. Berg (Ed.), Wettability, Dekker, New York, 1993, p. 311.
[30] J.G. Petrov, J. Ralston, M. Schneemilch, R. Hayes, J. Phys. Chem. B 107 (2003) 1634.
[31] J.G. Petrov, J. Ralston, M. Schneemilch, R. Hayes, Langmuir 19 (2003) 2795.
[32] C. Shen, D.W. Ruth, Phys. Fluids 10 (1998) 789.
[33] J.-D. Chen, N. Wada, J. Colloid Interface Sci. 148 (1998) 207.
[34] G.D. Yarnold, B.J. Mason, Proc. Phys. Soc. B 62 (1949) 121.
[35] R.L. Hoffman, J. Colloid Interface Sci. 50 (1975) 228.
[36] T.D. Blake, J. De Coninck, Adv. Colloid Interface Sci. 96 (2002) 21.
[37] W.H. Press, S.A. Teukolsky, W.T. Vetterling, B.P. Flannery, Numerical Recipes in Fortran, second ed., Cambridge Univ. Press, Cambridge, 1992.
[38] A. Prevost, E. Rolley, E.C. Guthmann, Phys. Rev. Lett. 83 (1999) 348.
[39] P.G. Petrov, J.G. Petrov, Langmuir 8 (1992) 1762.
[40] F. Brochard-Wyart, P.G. de Gennes, Adv. Colloid Interface Sci. 39 (1992) 1.
[41] M.J. de Ruijter, J. De Coninck, G. Oshanin, Langmuir 15 (1999) 2209.
[42] M.J. de Ruijter, M. Charlot, M. Voué, J. De Coninck, Langmuir 16 (2000) 2363.
[43] (a) Y.D. Shikhmurzaev, J. Multiphase Flow 19 (1993) 589;
(b) Y.D. Shikhmurzaev, Fluid Dyn. Res. 13 (1994) 45.
[44] J. Eggers, R. Evans, J. Colloid Interface Sci. 280 (2004) 537, and the response: Y.D. Shikhmurzaev, T.D. Blake, J. Colloid Interface Sci. 280 (2004) 539.
[45] T.D. Blake, Y.D. Shikhmurzaev, J. Colloid interface Sci. 253 (2002) 196.
[46] E.B. Dussan V, S.H. Davis, J. Fluid Mech. 65 (1974) 71.
[47] M.C.T. Wilson, J.L. Summers, P.H. Gaskell, Y.D. Shikhmurzaev, in: A.C. King, Y.D. Shikhmurzaev (Eds.), IUTAM Symp. Free Surface Flows (Birmingham, 2000), in: Fluid Mechanics and its Applications, vol. 62, Kluwer, Dordrecht, 2001, p. 345.
[48] M. Fermigier, P. Jenffer, J. Colloid Interface Sci. 146 (1991) 226.
[49] J. Eggers, Phys. Rev. Lett. 93 (2004) 094502-1.
[50] M.Y. Zhou, P. Sheng, Phys. Rev. Lett. 64 (1990) 882.
[51] T.D. Blake, Colloids Surf. 47 (1990) 135.
[52] G. Saville, Faraday II 73 (1997) 1122.
[53] J. Koplik, J.R. Banavar, J.F. Willemsen, Phys. Rev. Lett. 60 (1988) 1282.
[54] J. Koplik, J.R. Banavar, J.F. Willemsen, Phys. Fluids A 1 (1989) 781.
[55] P.A. Thompson, M.O. Robbins, Phys. Rev. Lett. 63 (1989) 766.
[56] P.A. Thompson, W.B. Brinckerhoff, M.O. Robbins, J. Adhesion Sci. Technol. 7 (1993) 535.
[57] D.R. Heine, G.S. Grest, E.B. Webb III, Phys. Rev. E 68 (2003) 061603-1.
[58] D.R. Heine, G.S. Grest, E.B. Webb III, Phys. Rev. E 70 (2004) 011606-1.
[59] G. Martic, F. Gentner, D. Seveno, D. Coulon, J. De Coninck, T.D. Blake, Langmuir 18 (2002) 7971.
[60] G. Martic, F. Gentner, D. Seveno, J. De Coninck, T.D. Blake, J. Colloid Interface Sci. 270 (2004) 171.
[61] D. Seveno, Thesis, Centre de Recherche en Modélisation Moléculaire and Faculté Polytechnique de Mons, Belgium, 2004.
[62] H. Benkreira, M. Khan, R. Patel, in: 12th International Coating Science and Technology Symposium, Rochester, NY, USA, 2004.